THE JOURNAL OF BIOLOGICAL CHEMISTRY VOL. 285, NO. 32, pp. 24487–24493, August 6, 2010

Mice with Tissue Inhibitor of Metalloproteinases 4 (*Timp4*) Deletion Succumb to Induced Myocardial Infarction but Not to Cardiac Pressure Overload*[S]

Received for publication, April 22, 2010, and in revised form, May 24, 2010 Published, JBC Papers in Press, June 1, 2010, DOI 10.1074/jbc.M110.136820

Ilpo Koskivirta[‡§¶1,2], Zamaneh Kassiri[§1], Otto Rahkonen[‡‖], Riku Kiviranta[‡], Gavin Y. Oudit[**], Trevor D. McKee[§3], Ville Kytö[¶], Antti Saraste[¶], Eero Jokinen[‖], Peter P. Liu[**], Eero Vuorio[‡], and Rama Khokha[§4]

From the [‡]Department of Medical Biochemistry and Genetics, University of Turku, FI-20520 Turku, Finland, the [§]Ontario Cancer Institute, Toronto, Ontario M5G 2M9, Canada, the [‖]Department of Pediatrics, University of Helsinki, Helsinki, FI-00029 HUS, Finland, the [**]Division of Cardiology, University of Toronto, Toronto, Ontario M5G 2N2, Canada, and the [¶]Department of Medicine, Turku University Hospital, FI-20521 Turku, Finland

Tissue inhibitor of metalloproteinases 4 (TIMP4) is expressed highly in heart and found dysregulated in human cardiovascular diseases. It controls extracellular matrix remodeling by inhibiting matrix metalloproteinases (MMPs) and is implicated in processes including cell proliferation, apoptosis, and angiogenesis. *Timp4*-deficient mice (*Timp4*$^{-/-}$) were generated to assess TIMP4 function in normal development and in models of heart disease. We deleted exons 1–3 of the *Timp4* gene by homologous recombination. *Timp4*$^{-/-}$ mice are born healthy, develop normally, and produce litters of normal size and gender distribution. These mice show no compensation by overexpression of *Timp1*, *Timp2*, or *Timp3* in the heart. Following cardiac pressure overload by aortic banding, *Timp4*$^{-/-}$ mice have comparable survival rate, cardiac histology, and cardiac function to controls. In this case, *Timp4* deficiency is compensated by increased cardiac *Timp2* expression. Strikingly, the induction of myocardial infarction (MI) leads to significantly increased mortality in *Timp4*$^{-/-}$ mice primarily due to left ventricular rupture. The post-MI mortality of *Timp4*$^{-/-}$ mice is reduced by administration of a synthetic MMP inhibitor. Furthermore, combining the genetic deletion of *Mmp2* also rescues the higher post-MI mortality of *Timp4*$^{-/-}$ mice. Finally, *Timp4*$^{-/-}$ mice suffer reduced cardiac function at 20 months of age. *Timp4* is not essential for murine development, although its loss moderately compromises cardiac function with aging. *Timp4*$^{-/-}$ mice are more susceptible to MI but not to pressure overload, and TIMP4 functions in its capacity as a metalloproteinase inhibitor after myocardial infarction.

Tissue inhibitors of metalloproteinases (TIMPs)[5] comprise a family of four endogenous inhibitors. Classically, matrix metalloproteinases (MMPs) and TIMPs are known as important regulators of extracellular matrix turnover during physiologic and numerous pathologic processes. Several other functions also have been ascribed to MMPs, many of which extend to their inhibitors (1). TIMPs also exhibit functions that appear to be independent of their metalloproteinase inhibitory capacity (2).

TIMP4 is the most recently discovered member of the TIMP family. It inhibits several soluble MMPs (types 1, 2, 3, 7, 8, 9, 12, 13, 19, and 26) and membrane-type MMPs (MT1, MT2, and MT3) (3–7). TIMP4 also inhibits a disintegrin and metalloproteinase (ADAM) 28 and ADAM33 (7) but not ADAM10 (which is inhibited by TIMP1 and TIMP3) or ADAM17 (which is inhibited only by TIMP3) (2, 7, 8). Inhibition of the ADAMTS (ADAM with thrombospondin motifs) family by TIMP4 has not yet been reported. Although *Timp* genes *1*, *2*, and *3* are widely expressed, the *Timp4* gene exhibits a restricted tissue expression pattern, with the highest expression in the heart, followed by brain, ovary, and skeletal muscle, and TIMP4 protein is detectable in the serum (9–11). Several lines of evidence suggest a specific role in cardiovascular pathology: *Timp4* is induced following endothelial injury of rat carotid artery (12); experimental ischemia-reperfusion injury results in the immediate release of TIMP4 from the myocardium (13); and down-regulation of *Timp4* is a common finding in animal models of heart failure (14–16) or myocardial infarction (17, 18). Similar observations have been observed in patients with ischemic cardiomyopathy (19).

To understand the functions of TIMP4 in the whole organism, we generated *Timp4* knock-out mice. Mice lacking other *Timp* genes develop normally at the gross level and can reproduce, *Timp1* knock-outs (20) exhibit impaired fertility (21), unfavorable changes in heart geometry (22), and resistance to bacterial infections (23, 24); *Timp2* knock-outs (25) or mice producing truncated TIMP2 (26) demonstrate reduced pro-MMP2 activation. Behavioral and motor phenotypes subsequently were characterized in *Timp2*-deficient mice (27, 28).

* This work was supported by research grants from the Academy of Finland, the Canadian Institutes of Health Research, and the Heart and Stroke Foundation of Canada.

[S] The on-line version of this article (available at http://www.jbc.org) contains supplemental methods, Tables 1 and 2, Figs. 1–5, and additional references.

[1] Both authors contributed equally to this work.

[2] Recipient of personal research grants from the Finnish Medical Foundation and a training grant from Turku Graduate School of Biomedical Sciences (TuBS).

[3] Supported by a Susan G. Komen Postdoctoral Fellowship.

[4] To whom correspondence should be addressed: Ontario Cancer Institute, 610 University Ave., 10-330, Toronto, ON M5G 2M9. Tel.: 416-946-2051; Fax: 416-946-2984; E-mail: rkhokha@uhnres.utoronto.ca.

[5] The abbreviations used are: TIMP, tissue inhibitor of metalloproteinases; MMP, matrix metalloproteinase; AB, aortic banding; ADAM, a distintegrin and metalloproteinase; ADAMTS, a disintegrin and metalloproteinase with thrombospondin motifs; LAD, left anterior descending coronary artery; LV, left ventricular; MI, myocardial infarction; MMPi, matrix metalloproteinase inhibitor; RT, reverse transcription; ANP, atrial natriuretic peptide; BNP, natriuretic peptide B.

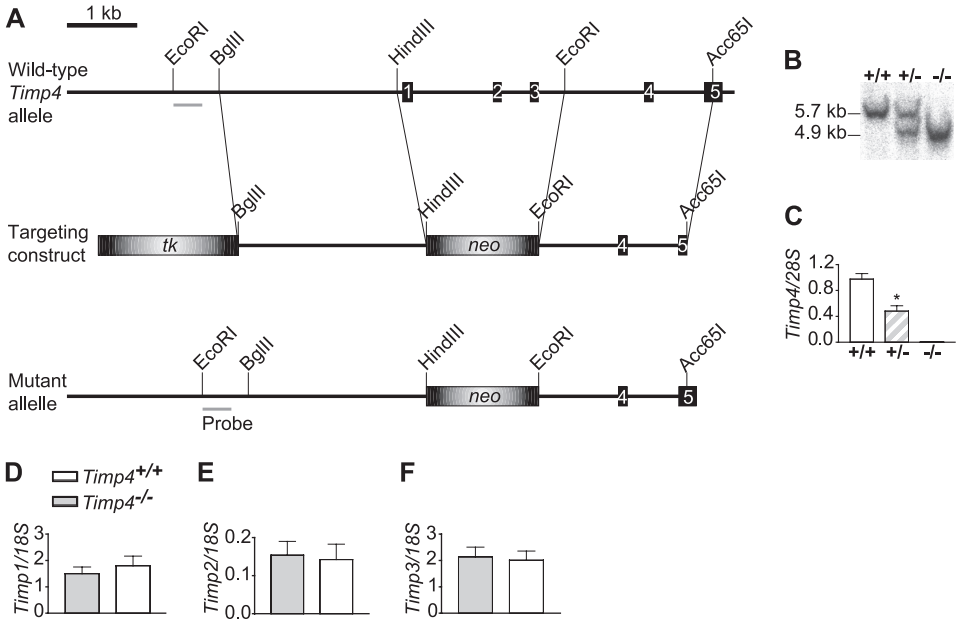

FIGURE 1. **Targeting the *Timp4* gene.** *A*, the targeting construct was produced by cloning genomic BglII-HindIII and EcoRI-Acc65I fragments of the murine *Timp4* gene into pKO Scrambler 921, which contains neomycin (*neo*) and thymidine kinase (*tk*) cassettes. The mutant allele lacks the first three exons. *B*, Southern blot analysis of genomic DNA after EcoRI digestion, hybridized with a 5′-probe, showing the 5.7-kb wild-type and the 4.9-kb mutant fragments. *C*, the histogram shows quantification of Northern analysis (see supplemental Fig. 1) of adult cardiac tissue revealing a lack of *Timp4* mRNA in homozygous mice, and 50.7% reduction of *Timp4* mRNA in heterozygous mice (mean ± S.E.; *, $p < 0.001$ *versus* *Timp4*$^{+/+}$). *D–F*, Taqman RT-PCR analysis of RNA for *Timp1*, *Timp2*, and *Timp3* in hearts of *Timp4*$^{+/+}$ and *Timp4*$^{-/-}$ mice. Values were normalized to 18 S rRNA and are expressed as mean ± S.E.; $n = 4–6$ for each group.

Timp3 knock-out mice have accelerated post-lactation mammary gland involution (29) and develop spontaneous air space enlargement in the lungs (30). In addition, these mice exhibit abnormal processing of tumor necrosis factor α (31), compromised heart function with aging (32), and increased susceptibility to aortic banding (AB) (33). Here, we show that *Timp4*-deficient mice develop and reproduce normally but are prone specifically to fatal ventricular wall rupture after myocardial infarction (MI), a pathology blocked by a synthetic MMP inhibitor or by the deletion of *Mmp2*.

EXPERIMENTAL PROCEDURES

Generation of Knock-out Mice—A knock-out construct with neomycin resistance and thymidine kinase selection cassettes was designed to delete a 2.4-kb genomic fragment containing exons 1–3 of the *Timp4* gene (9). This deletes translation initiation codon (atg) and is predicted to eliminate transcription initiation.

Phenotypic Analyses—For analyses of aged mice, *Timp4*$^{-/-}$ mice were kept on outbred C57BL/6 × 129SvEv background. RNA analyses were performed using Northern blotting and real-time Taqman® RT-PCR. Cardiac hydroxyproline was determined by a modified Woessner's protocol.

Functional Studies of the Cardiovascular System—The systolic blood pressures and heart rates of 5-month-old, unanesthetized, male *Timp4*$^{+/+}$ ($n = 9$) and *Timp4*$^{-/-}$ ($n = 5$) mice were measured using a tail-cuff method (TSE Blood Pressure Measuring System 209000-9002-1, TSE Systems GmbH, Bad Homburg, Germany) on a temperature-controlled platform. Before measurements, restrained mice were trained to inflating and deflating tail cuff. Blood flow in caudal arteries was monitored by a pulse transducer, whereas arteries were occluded gradually by an inflating pressure cuff. Systolic arterial pressure equals the pressure in tail cuff when blood flow became undetectable by sensor. Heart rate was obtained by continuous monitoring of pulse signal. For each mouse, at least 30 consecutive measurements were performed. Unreliable measurements, containing for example movement artifacts, were discarded and the average of remaining measurements (20 to 25 per mouse) was used for statistical analyses.

For *in vivo* echocardiographic measurements, 20-month-old male *Timp4*$^{-/-}$ mice ($n = 6$) and control littermates ($n = 4$) were anesthetized with diazepam (10 mg/kg) and ketamine (60 mg/kg) and studied by transthoracic Doppler echocardiography using Acuson Sequoia 512 (Siemens Acuson, Mountain View, CA) with a 15-MHz linear transducer. Left ventricular dimensions and mass and fractional shortening were measured in short axis M mode images of the left ventricle (34). Myocardial performance index, a sensitive Doppler-based measure of global left ventricular function was calculated from time intervals obtained from transmitral inflow and aortic outflow (35). To assess diastolic function, ratio of transmitral flow velocity during early and late diastole (E/A ratio) was calculated. Coronary microvascular function was assessed by measuring coronary flow reserve in the middle part of descending left coronary artery. Coronary flow reserve was calculated as the ratio of peak diastolic flow velocity during maximal vasodilatation induced by adenosine (0.32 mg/kg/min) to resting flow velocity (36). Cardiac function measurements following pressure overload or myocardial infarction were performed under light isoflurane anesthesia (0.75%) by echocardiography and *in vivo* hemodynamic measurements (33).

Mice (*Timp4*$^{+/+}$ and *Timp4*$^{-/-}$) used in pressure overload and myocardial infarction studies were of C57Bl background, derived by six back-crossings into this strain. Pressure overload was subjected to male *Timp4*$^{-/-}$ and control mice at the age of 8 weeks by performing constriction of descending aorta as described earlier (33). Briefly, mice were anesthetized with ketamine-xylazine, intubated, and ventilated with rodent ventilator. During surgery, descending aorta was identified, and a ligature was tied around descending aorta, and a 27-gauge needle was placed parallel to it. Next, the needle was removed, but the ligature was left, causing constant and permanent constriction of aorta. The thorax was closed, and mice were monitored for up to 12 weeks. Sham-operated mice underwent similar operation except that the ligation of aorta was not tightened, and it

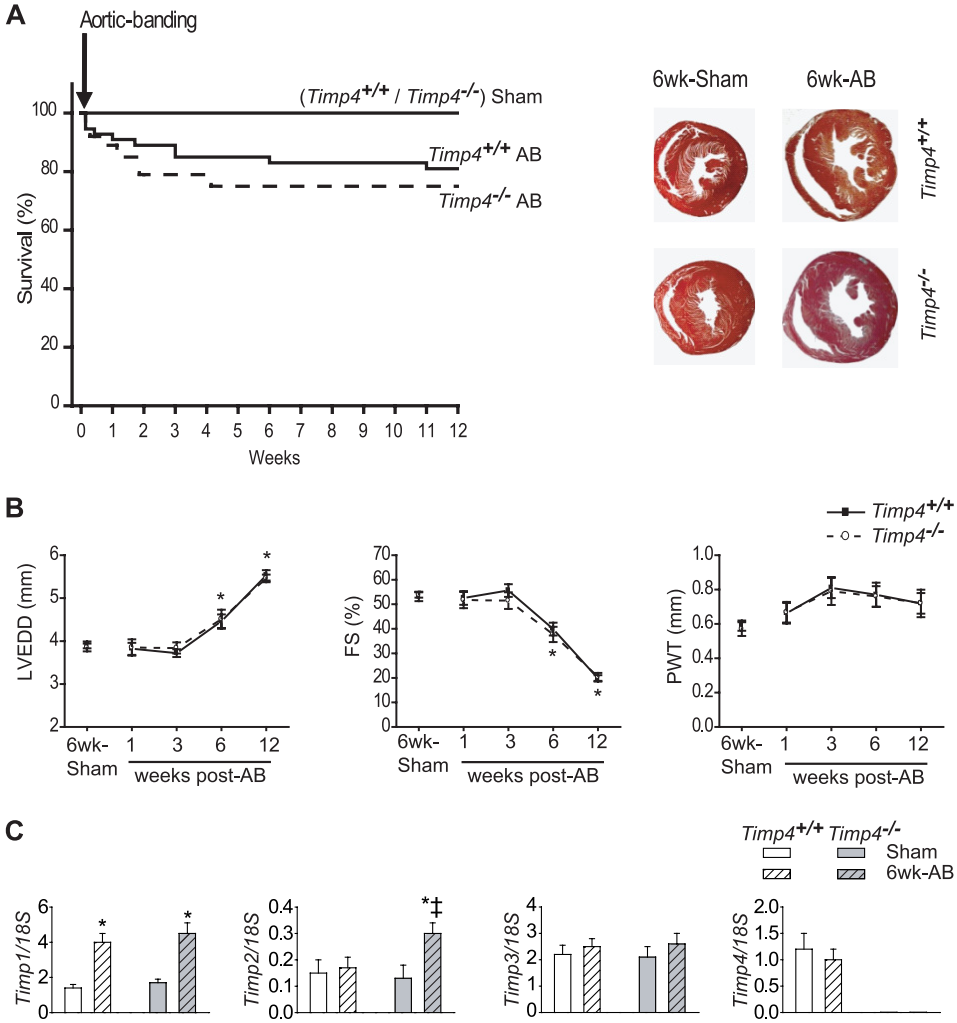

FIGURE 2. **The loss of TIMP4 did not impact the cardiac response to pressure overload.** *A*, survival of AB- or sham-operated *Timp4*$^{+/+}$ and *Timp4*$^{-/-}$ mice ($n = 20$/group), and representative macroscopic heart cross-sections at 6-weeks post-AB. *B*, left ventricular end-diastolic dimension (*LVEDD*), fractional shortening (*FS*) and posterior wall thickness (*PWT*) are equivalent in these mice up to 12-weeks post-AB. Data are mean ± S.E.; $n = 3$, sham groups; $n = 6$, AB groups; *, $p < 0.05$ *versus* corresponding sham group. *C*, Taqman RT-PCR analysis of RNA for *Timp1*, *Timp2*, *Timp3*, and *Timp4* in hearts of *Timp4*$^{+/+}$ and *Timp4*$^{-/-}$ mice at 6 weeks after sham operation or aortic banding. Values were normalized to 18 S rRNA and are expressed as mean ± S.E.; $n = 4–6$ for each group. *, $p < 0.05$ *versus* corresponding sham; ‡, $p < 0.05$ *versus* *Timp4*$^{+/+}$ AB.

was removed before closure of thorax. At 1, 3, 6, and 12 weeks after aortic-banding, cardiac function was monitored by echocardiography as described (33).

10–12-week-old *Timp4*$^{+/+}$ and *Timp4*$^{-/-}$ male mice were subjected to myocardial infarction by left anterior descending coronary artery (LAD) ligation (37) or to sham operation. Briefly, mice were anesthetized with ketamine-xylazine, intubated, and ventilated with rodent ventilator. Thorax and pericardium were opened to expose LAD, which was ligated. Then, chest was closed, and mice were monitored up to 7 days. Heart function was evaluated on surviving mice by echocardiography and *in vivo* hemodynamics before sacrifice for tissue collection (33). The synthetic MMP inhibitor PD166793 (Pfizer, Inc.) was administered daily (25 mg/kg) by gavage, starting 1 week before MI until the mice were euthanized.

Generation of the knock-out mice and phenotypic analyses of aged mice were performed under protocols approved by the Institutional Committee for Animal Welfare (University of Turku, Turku, Finland). The AB and MI protocols were approved by the Ontario Cancer Institute Animal Care Committee (Toronto, Canada) in accordance with guidelines of the Canadian Council for Animal Care.

Second Harmonic Generation Imaging—For visualization of fibrillar collagen *in vivo*, second harmonic and autofluorescence was captured on a Zeiss LSM 510 META NLO microscope, using a C-Apo 40×/1.2 NA objective lens. Intact hearts were isolated, immersed in phosphate-buffered saline, and imaged through a glass coverslip. Excitation was provided by a Chameleon femtosecond pulsed laser tuned to 840 nm, and second harmonic generation signal was collected via epidetection through a 425/35 bandpass filter, with the autofluorescence signal collected simultaneously through a 525/25 bandpass filter. The nature of the second harmonic signal was confirmed by spectral analysis using a META detector, showing a narrow peak corresponding to half the wavelength of the input excitation. Image volumes were collected in infarct and peri-infarct regions, and maximum intensity projections of regions of interest were generated using NIH ImageJ software. Additional methods can be found in the supplemental material.

RESULTS

Generation of Timp4 Knock-out Mice—Electroporation of the targeting construct (Fig. 1*A*) into embryonic stem cells resulted in 216 clones, which were screened by Southern blotting. One clone harboring the correct targeting event was identified by the presence of a 4.9-kb mutant band in addition to the wild-type band (Fig. 1*B*). Injection of targeted embryonic stem cells into blastocysts gave rise to four high percentage chimeric males, of which two frequently produced heterozygous pups. To confirm that the mutant *Timp4* allele did not produce any *Timp4* mRNA, total heart RNA from animals of the three genotypes was analyzed by Northern blotting for *Timp4* mRNA expression (supplemental Fig. 1). Heterozygous mice had 50.7% ($p < 0.001$; $n = 9$; Fig. 1*C*) of the mRNA levels seen in control littermates for the major 1.1-kb *Timp4* transcript. No *Timp4* mRNA was detected in *Timp4*$^{-/-}$ ($n = 5$) mice. These observations were confirmed by RT-PCR (data not shown). Breeding of the *Timp4*-deficient mice resulted in litters of normal size and gender distribution (supplemental Table 1).

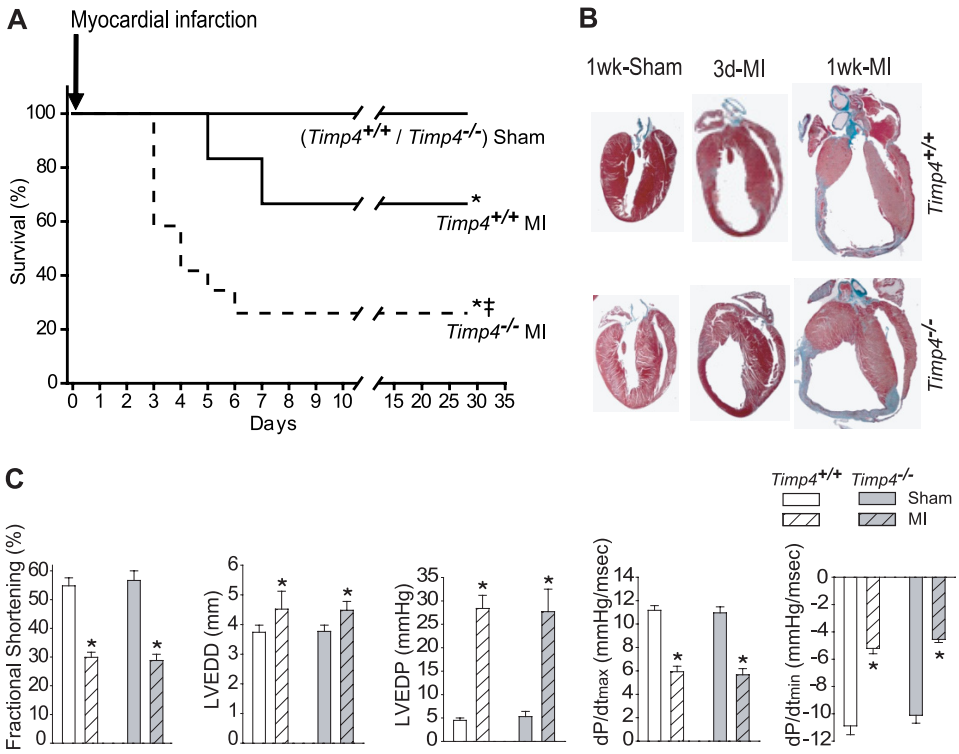

FIGURE 3. **Timp4$^{-/-}$ mice experience significantly higher mortality following MI.** *A*, rupture-related survival of *Timp4*$^{+/+}$ and *Timp4*$^{-/-}$ mice following MI or sham operation; $n = 27$ for *Timp4*$^{-/-}$ MI and $n = 20$ for *Timp4*$^{+/+}$ MI; *, $p < 0.05$ *versus* sham; ‡, $p < 0.05$ *versus Timp4*$^{+/+}$ MI. *B*, representative macroscopic cross-sectional images of *Timp4*$^{+/+}$ and *Timp4*$^{-/-}$ hearts at indicated times after sham operation or MI. *C*, functional and structural analyses showing fractional shortening, LV end-diastolic dimension (*LVEDD*), LV end-diastolic pressure (*LVEDP*), and LV peak rates of pressure-rise and pressure-fall (±dP/dt) in mice at 1-week post-sham or post-MI. Data represent mean ± S.E.; $n = 6$/group; *, $p < 0.05$ *versus* corresponding sham group.

Characterization of the Cardiac Structure and Function in Timp4$^{-/-}$ *Mice*—As the literature suggests a role for TIMP4 in heart, cardiac tissue of *Timp4*$^{-/-}$ mice was investigated at the age of 5 months. Measurement of body weights and heart-to-body weight ratios in *Timp4*$^{-/-}$ and *Timp4*$^{+/+}$ mice revealed no differences (supplemental Table 2). Neither were any statistically significant differences observed in blood pressure or heart rate in 5-month-old knock-out and control mice (supplemental Table 2). Furthermore, histologic evaluation of the heart at 5 months of age showed no differences in the cardiomyocyte size (supplemental Table 2) or the amount of collagen (data not shown) as indicated by trichrome staining. Determination of the hydroxyproline content in cardiac collagen showed essentially identical levels between *Timp4*$^{-/-}$ ($n = 8$) and control mice ($n = 4$; 1.80 ± 0.05 *versus* 1.81 ± 0.08 μg/mg) at the age of 5 months. Taqman RT-PCR analyses showed that the cardiac mRNA levels of *Timp* genes 1, 2, and 3 remained comparable between *Timp4*$^{+/+}$ and *Timp4*$^{-/-}$ mice (Fig. 1, *D–F*).

Timp4 Deficiency Does Not Affect Survival or Heart Dysfunction Following Pressure Overload—To investigate the effects of a *Timp4* deficiency on chronic pressure overload, *Timp4*$^{-/-}$ and control mice were subjected to aortic banding at the age of 8 weeks. The survival rates were similar over the next 12 weeks (Fig. 2*A*). Echocardiography at 1, 3, 6, and 12 weeks post-AB, showed comparable cardiac function in *Timp4*-deficient and control mice (Fig. 2*B*). Histological evaluation of cardiac hypertrophy and fibrosis at 6 weeks did not reveal any differences (data not shown). Moreover, the expression levels of the natriuretic peptides (atrial natriuretic peptide, ANP, and natriuretic peptide B, BNP), as well as collagen types I and III, were comparable in *Timp4*$^{+/+}$ and *Timp4*$^{-/-}$ hearts (data not shown). We then determined whether the lack of post-AB phenotype might be due to compensatory mechanisms involving other *Timp* genes. In contrast to control mice, we observed a 1.6-fold ($p < 0.05$) increase in cardiac *Timp2* expression in *Timp4*-deficient mice at 6 weeks post-AB (Fig. 2*C*), whereas the expression levels of *Timp1* and *Timp3* remained comparable between genotypes.

Timp4 Loss Increases Mortality after Myocardial Infarction—To further characterize the significance of TIMP4 in heart disease, *Timp4* knock-out mice were subjected to experimental myocardial infarction induced by LAD ligation. This is known to result in severe morbidity by large myocardial infarct and progressive left ventricular (LV) dilation (Fig. 3*B*). *Timp4*$^{-/-}$ mice showed significantly increased mortality in comparison with *Timp4*$^{+/+}$ mice after MI between days 3 to 7 (Fig. 3*A*; supplemental Fig. 2). In autopsy, a LV wall rupture was identified as the cause of death in the majority of cases in both genotypes (Fig. 4*A*). By echocardiography and *in vivo* hemodynamics, we observed a decrease in fractional shortening, an increase in LV end-diastolic diameter and pressure, and suppressed LV peak rates of pressure-rise and pressure-fall in mice at 7 days after MI (Fig. 3*C*). These studies indicated severely deteriorated LV function post-MI, but the extent of this dysfunction was comparable between genotypes. Thus, *Timp4*$^{-/-}$ mice exhibit greater mortality, but those that recover have deterioration of heart function similar to controls.

Cardiac Collagen Network Is Compromised in Timp4-deficient Mice Post-MI—The structure of the cardiac collagen network was evaluated as a possible cause for increased rupture in *Timp4*$^{-/-}$ mice post-MI. The fibrillar collegen network was visualized alongside cellular autofluorescence using combined second harmonic generation and multiphoton fluorescence microscopy. In *Timp4*-deficient mice, the fibrillar collagen network is compromised as indicated by reduced collagen fiber intensity (Fig, 4, *B–F*). Expression analysis of major cardiac collagens (types I and III) revealed reduced collagen synthesis at 3 and 7 days post-MI (Fig, 4*G*). Further, synthesis of *Timp* genes and major gelatinases and collagenases were analyzed at 7 days post-MI. Expression of *Timp1–3* genes were comparable in *Timp4*-deficient and control mice (data not shown). In zymog-

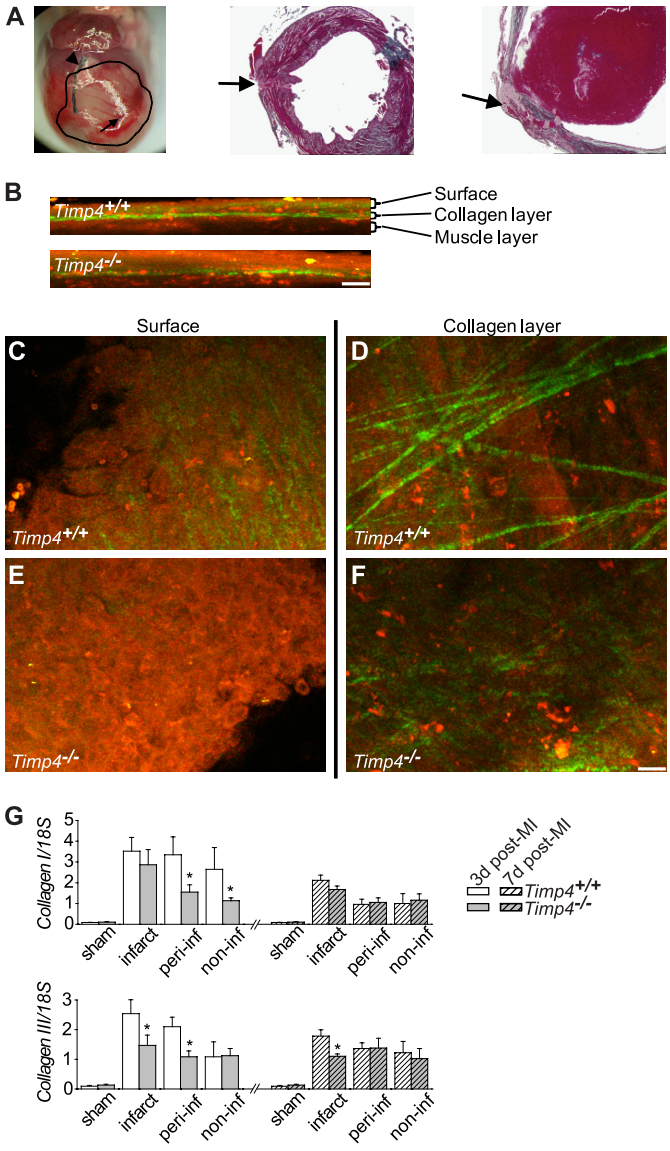

FIGURE 4. **Cardiac rupture and decreased collagen synthesis and disruption of collagen network in *Timp4*$^{-/-}$ hearts after MI.** *A*, a representative picture of a ruptured heart following MI and trichrome-stained fixed LV tissue sections showing the rupture area (*arrow*) and LAD ligation (*arrowhead*). The infarct area is marked with a *dotted line*. *B–F*, second harmonic generation (*green pseudocolor*) and multiphoton fluorescence (*red pseudocolor*) images indicating compromised fibrillar collagen and altered cellularity in *Timp4*-deficient hearts post-MI. *B*, the depth profile extending below the heart surface. *C–F*, 10-μm-thick maximum intensity projections of the surface and collagen layers of *Timp4*$^{+/+}$ and *Timp4*$^{-/-}$ heart infarct regions. *Scale bar*, 20 μm (*B–F*). *G*, Taqman RT-PCR analysis of RNA for collagen I and III in hearts of *Timp4*$^{+/+}$ and *Timp4*$^{-/-}$ mice at 3 and 7 (*dashed bars*) days after sham operation or myocardial infarction. Values were normalized to 18 S rRNA and are expressed as mean ± S.E.; $n = 4-6$ for each group. *, $p < 0.05$ *versus* *Timp4*$^{+/+}$ MI. *peri-inf*, peri-infarct; *non-inf*, noninfarct.

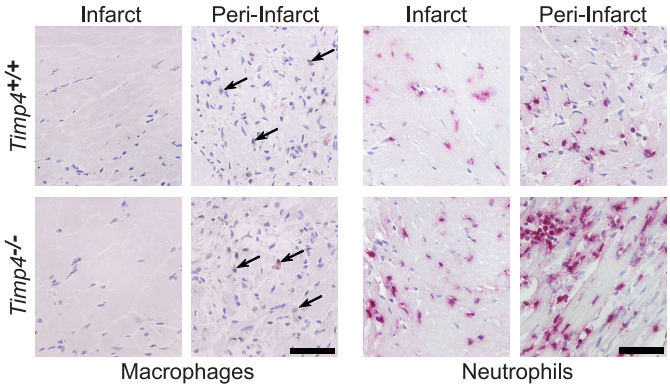

FIGURE 5. **Increased neutrophil accumulation in *Timp4*$^{-/-}$ hearts at 3 days post-MI.** Immunodetection of macrophages (*arrow*) and neutrophils in infarct and peri-infarct areas of *Timp4*$^{+/+}$ and *Timp4*$^{-/-}$ hearts. *Scale bar*, 50 μm.

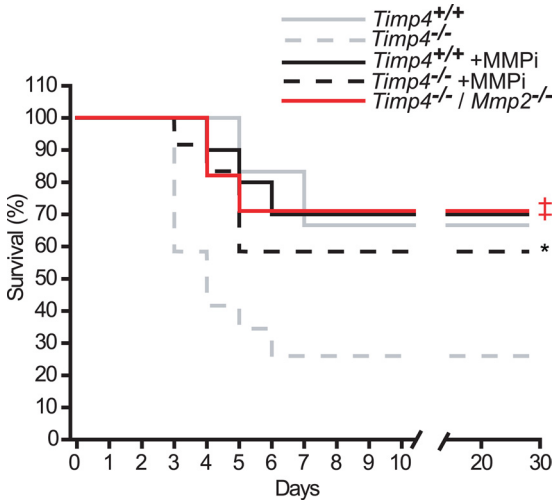

FIGURE 6. **Improved post-MI survival in *Timp4*$^{-/-}$ mice following MMPi treatment or deletion of *Mmp2*.** The graph shows the rupture-related post-MI survival of *Timp4*$^{+/+}$ (*solid line*) and *Timp4*$^{-/-}$ (*dashed line*) mice that did not receive additional treatment (*gray*; data from Fig. 3) or mice treated with MMPi (black; $n = 9$ for *Timp4*$^{+/+}$ +MMPi; $n = 11$ for *Timp4*$^{-/-}$ +MMPi; *, $p < 0.05$ *versus* untreated *Timp4*$^{-/-}$ mice). A *red solid line* represents *Timp4/Mmp2* double knock-out mice ($n = 10$, ‡, $p < 0.05$ *versus* *Timp4*$^{-/-}$ mice without MMPi treatment).

raphy, gelatinase activity of the cardiac tissue was comparable between genotypes at 3 days post-MI (supplemental Fig. 3).

Neutrophil Accumulation Is Increased in Timp4$^{-/-}$ *Hearts Post-MI*—After MI, a controlled inflammatory process takes place to replace necrotic areas with scar tissue. Multiphoton fluorescence microscopy suggested increased cellularity in *Timp4*$^{-/-}$ cardiac tissue (Fig. 4, *B*, *C*, and *E*). Possibly altered inflammatory cell accumulation was investigated by immunohistochemistry in *Timp4*-deficient and control hearts at 3 days post-MI. Staining of macrophages indicated a slight increase in macrophage numbers in *Timp4*$^{-/-}$ hearts, but quantification was not feasible because of low intensity of staining (Fig. 5). In *Timp4*-deficient hearts, accumulation of neutrophils was significantly increased in infarct, peri-infarct, and noninfarct areas when compared with *Timp4*$^{+/+}$ MI hearts (Fig. 5). In contrast, angiogenesis seemed to be similar in *Timp4*$^{-/-}$ and *Timp4*$^{+/+}$ mice as indicated by CD31 staining (supplemental Fig. 4).

MMPi Treatment or the Genetic Ablation of Mmp2 Reduces the Post-MI Mortality of Timp4$^{-/-}$ *Mice*—To test whether the poor post-MI survival was related to the loss of MMP inhibitory function in the *Timp4*$^{-/-}$ heart, a broad spectrum MMP-specific inhibitor (PD166793; MMPi) was orally administered to *Timp4*-deficient and control MI-mice as described previously (33). MMPi treatment did not affect the post-MI survival rate of *Timp4*$^{+/+}$ mice; however, the excessive lethality seen in *Timp4*$^{-/-}$ mice was rescued by MMPi treatment, making the survival rate of MMPi-treated *Timp4*$^{-/-}$ mice comparable with *Timp4*$^{+/+}$ mice (Fig. 6). Earlier studies have shown a

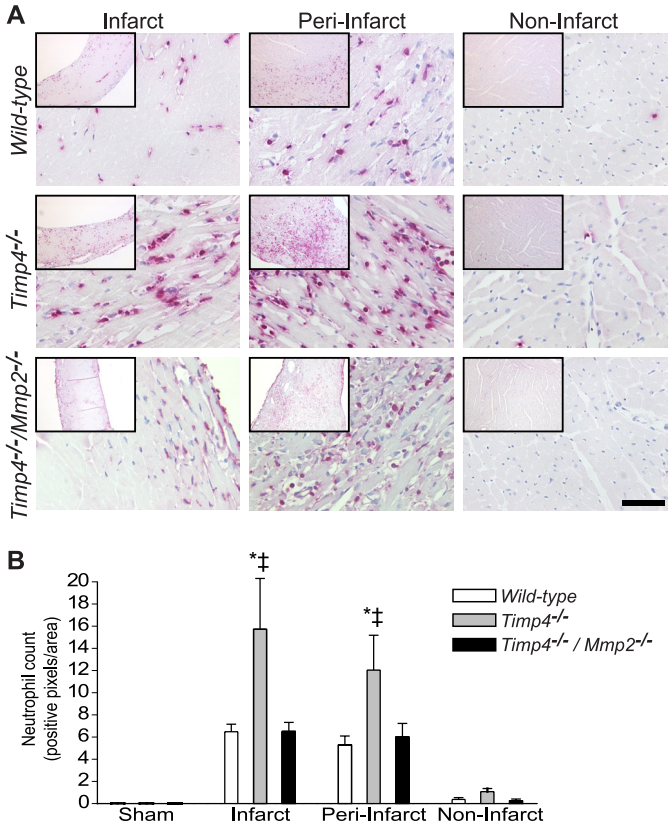

FIGURE 7. **Increased cardiac neutrophil accumulation of *Timp4*-deficient mice post-MI is normalized by ablation of *Mmp2*.** *A*, neutrophil staining of *Timp4*$^{+/+}$, *Timp4*$^{-/-}$, and double knock-out (*Timp4*$^{-/-}$/*Mmp2*$^{-/-}$) cardiac tissue at 3 days following MI. *Scale bar*, 50 μm. *B*, histomorphometric quantification of neutrophils in cardiac tissue post-MI. Values expressed as mean ± S.E., *, $p < 0.05$ *versus* wild-type control in same group; ‡, $p < 0.05$ *versus* double knock-out in same group.

reduction in post-MI rupture rates in *Mmp2* knock-out mice (38, 39). An *Mmp2* deficiency was crossed into the model and the double-deficient *Timp4*$^{-/-}$/*Mmp2*$^{-/-}$ mice were observed to have a post-MI survival rate (Fig. 6) similar to controls. Moreover, the accumulation of neutrophils in *Timp4*$^{-/-}$/*Mmp2*$^{-/-}$ hearts post-MI was now comparable with control mice (Fig. 7, *A* and *B*).

Cardiac Function Is Moderately Compromised in Aged Timp4$^{-/-}$ *Mice*—To determine the effect of aging on heart structure and function of *Timp4*$^{-/-}$ and *Timp4*$^{+/+}$ mice, *in vivo* echocardiography was performed at the age of 20 months. Impaired heart function in *Timp4* knock-out mice was evident by a poor myocardial performance index (supplemental Fig. 5), whereas the fractional shortening (41.9 ± 0.9 in *Timp4*$^{+/+}$ *versus* 45.8 ± 2.1% in *Timp4*$^{-/-}$) and E/A ratio (data not shown) were comparable between genotypes. Moreover, coronary flow reserve, a measurement of coronary microvascular function, was decreased in *Timp4*$^{-/-}$ mice (supplemental Fig. 5). Also, echocardiography demonstrated increased septal and posterior wall thickness (data not shown) accompanied by increased LV mass in *Timp4*-deficient mice (supplemental Fig. 5). Next, we asked whether this moderate dysfunction of *Timp4*$^{-/-}$ hearts was a reflection of aberrant cardiac fibrosis or myocardial hypertrophy. Myocyte cross-sectional area, assessed by histomorphometry, showed no differences between the genotypes (supplemental Fig. 5), and although increased fibrosis could be seen using Masson's trichrome staining in both genotypes as a function of age up to 20 months, the quantification of collagen by hydroxyproline assay did not reveal differences between control and *Timp4*$^{-/-}$ mice (supplemental Fig. 5).

DISCUSSION

High expression of *Timp4* mRNA in the heart (9, 10), animal models of heart disease (14, 15, 18), and in patients with cardiovascular pathology (11, 19) together suggest a specific role for TIMP4 in the development, physiology, and pathology of the cardiovascular system. Mice with a targeted deletion of *Timp4* exhibited normal development, we were able to observe a cardiac phenotype only in 20-month-old *Timp4* knock-out mice. In models of cardiac stress, our studies demonstrated that TIMP4 is essential during the healing response to myocardial infarction. This was not the case following aortic banding, where the induction of TIMP2 appears to compensate for the lack of TIMP4.

Cardiac TIMPs serve important functions, as gleaned from the use of *Timp*-null mice. *Timp1*$^{-/-}$ mice display altered LV geometry by 4 months of age (22), and *Timp3*$^{-/-}$ mice exhibit features of human dilated cardiomyopathy at 21 months but not earlier (32). In response to pressure overload, *Timp3* knock-outs develop heart failure, which is prevented by combining genetic deletion of tumor necrosis factor α with inhibition of MMPs (33). After MI, *Timp1* knock-outs show accelerated, MMP-dependent LV remodeling, without any effect on survival or LV rupture (40, 41). *Timp3*$^{-/-}$ knockouts have increased mortality and LV rupture within the first week of MI, as well as a greater cardiac dysfunction at 1–4 weeks post-MI (42). Here, we establish that *Timp4*$^{-/-}$ mice are specifically predisposed to LV rupture after MI, which is prevented by MMPi-treatment or the loss of *Mmp2*. A decrease in TIMP4 levels has been reported in animal models of MI (17, 18) and in cardiac patients (19, 43). The present study highlights TIMP4 as a critical regulator of MMP activity during the healing process following myocardial infarction.

Acknowledgments—We thank Merja Lakkisto and Tuula Oivanen for expert technical help. The Umeå Transgene Core Facility (Umeå University, Umeå, Sweden) is acknowledged for performing the blastocyst injections.

REFERENCES

1. Murphy, G., and Nagase, H. (2008) *Mol. Aspects Med.* **29,** 290–308
2. Lambert, E., Dassé, E., Haye, B., and Petitfrère, E. (2004) *Crit. Rev. Oncol. Hematol.* **49,** 187–198
3. Morrison, C. J., Butler, G. S., Bigg, H. F., Roberts, C. R., Soloway, P. D., and Overall, C. M. (2001) *J. Biol. Chem.* **276,** 47402–47410
4. Zhao, H., Bernardo, M. M., Osenkowski, P., Sohail, A., Pei, D., Nagase, H., Kashiwagi, M., Soloway, P. D., DeClerck, Y. A., and Fridman, R. (2004) *J. Biol. Chem.* **279,** 8592–8601
5. Stratmann, B., Farr, M., and Tschesche, H. (2001) *Biol. Chem.* **382,** 987–991
6. Stracke, J. O., Hutton, M., Stewart, M., Pendás, A. M., Smith, B., López-Otin, C., Murphy, G., and Knäuper, V. (2000) *J. Biol. Chem.* **275,** 14809–14816
7. Melendez-Zajgla, J., Del Pozo, L., Ceballos, G., and Maldonado, V. (2008)

Mol. Cancer **7,** 85
8. Amour, A., Knight, C. G., Webster, A., Slocombe, P. M., Stephens, P. E., Knäuper, V., Docherty, A. J., and Murphy, G. (2000) *FEBS Lett.* **473,** 275–279
9. Rahkonen, O. P., Koskivirta, I. M., Oksjoki, S. M., Jokinen, E., and Vuorio, E. I. (2002) *Biochim. Biophys. Acta* **1577,** 45–52
10. Leco, K. J., Apte, S. S., Taniguchi, G. T., Hawkes, S. P., Khokha, R., Schultz, G. A., and Edwards, D. R. (1997) *FEBS Lett.* **401,** 213–217
11. Koskivirta, I., Rahkonen, O., Mäyränpää, M., Pakkanen, S., Husheem, M., Sainio, A., Hakovirta, H., Laine, J., Jokinen, E., Vuorio, E., Kovanen, P., and Järveläinen, H. (2006) *Histochem Cell Biol.* **126,** 335–342
12. Dollery, C. M., McEwan, J. R., Wang, M., Sang, Q. A., Liu, Y. E., and Shi, Y. E. (1999) *Circ. Res.* **84,** 498–504
13. Schulze, C. J., Wang, W., Suarez-Pinzon, W. L., Sawicka, J., Sawicki, G., and Schulz, R. (2003) *Circulation* **107,** 2487–2492
14. Hoit, B. D., Takeishi, Y., Cox, M. J., Gabel, M., Kirkpatrick, D., Walsh, R. A., and Tyagi, S. C. (2002) *Mol. Cell Biochem.* **238,** 145–150
15. Li, H., Simon, H., Bocan, T. M., and Peterson, J. T. (2000) *Cardiovasc. Res.* **46,** 298–306
16. Seeland, U., Kouchi, I., Zolk, O., Itter, G., Linz, W., and Böhm, M. (2002) *J. Mol. Cell Cardiol.* **34,** 151–163
17. Mukherjee, R., Brinsa, T. A., Dowdy, K. B., Scott, A. A., Baskin, J. M., Deschamps, A. M., Lowry, A. S., Escobar, G. P., Lucas, D. G., Yarbrough, W. M., Zile, M. R., and Spinale, F. G. (2003) *Circulation* **107,** 618–625
18. Wilson, E. M., Moainie, S. L., Baskin, J. M., Lowry, A. S., Deschamps, A. M., Mukherjee, R., Guy, T. S., St John-Sutton, M. G., Gorman, J. H., 3rd, Edmunds, L. H., Jr., Gorman, R. C., and Spinale, F. G. (2003) *Circulation* **107,** 2857–2863
19. Li, Y. Y., Feldman, A. M., Sun, Y., and McTiernan, C. F. (1998) *Circulation* **98,** 1728–1734
20. Soloway, P. D., Alexander, C. M., Werb, Z., and Jaenisch, R. (1996) *Oncogene* **13,** 2307–2314
21. Nothnick, W. B. (2001) *Reproduction* **122,** 923–927
22. Roten, L., Nemoto, S., Simsic, J., Coker, M. L., Rao, V., Baicu, S., Defreyte, G., Soloway, P. J., Zile, M. R., and Spinale, F. G. (2000) *J. Mol. Cell Cardiol.* **32,** 109–120
23. Lee, M. M., Yoon, B. J., Osiewicz, K., Preston, M., Bundy, B., van Heeckeren, A. M., Werb, Z., and Soloway, P. D. (2005) *Infect. Immun.* **73,** 661–665
24. Osiewicz, K., McGarry, M., and Soloway, P. D. (1999) *Ann. N.Y. Acad. Sci.* **878,** 494–496
25. Wang, Z., Juttermann, R., and Soloway, P. D. (2000) *J. Biol. Chem.* **275,** 26411–26415
26. Caterina, J. J., Yamada, S., Caterina, N. C., Longenecker, G., Holmbäck, K., Shi, J., Yermovsky, A. E., Engler, J. A., and Birkedal-Hansen, H. (2000) *J. Biol. Chem.* **275,** 26416–26422
27. Jaworski, D. M., Boone, J., Caterina, J., Soloway, P., and Falls, W. A. (2005) *Brain Res.* **1051,** 81–89
28. Jaworski, D. M., Soloway, P., Caterina, J., and Falls, W. A. (2006) *J. Neurobiol.* **66,** 82–94
29. Fata, J. E., Leco, K. J., Voura, E. B., Yu, H. Y., Waterhouse, P., Murphy, G., Moorehead, R. A., and Khokha, R. (2001) *J. Clin. Invest.* **108,** 831–841
30. Leco, K. J., Waterhouse, P., Sanchez, O. H., Gowing, K. L., Poole, A. R., Wakeham, A., Mak, T. W., and Khokha, R. (2001) *J. Clin. Invest.* **108,** 817–829
31. Mohammed, F. F., Smookler, D. S., Taylor, S. E., Fingleton, B., Kassiri, Z., Sanchez, O. H., English, J. L., Matrisian, L. M., Au, B., Yeh, W. C., and Khokha, R. (2004) *Nat. Genet.* **36,** 969–977
32. Fedak, P. W., Smookler, D. S., Kassiri, Z., Ohno, N., Leco, K. J., Verma, S., Mickle, D. A., Watson, K. L., Hojilla, C. V., Cruz, W., Weisel, R. D., Li, R. K., and Khokha, R. (2004) *Circulation* **110,** 2401–2409
33. Kassiri, Z., Oudit, G. Y., Sanchez, O., Dawood, F., Mohammed, F. F., Nuttall, R. K., Edwards, D. R., Liu, P. P., Backx, P. H., and Khokha, R. (2005) *Circ. Res.* **97,** 380–390
34. Tanaka, N., Dalton, N., Mao, L., Rockman, H. A., Peterson, K. L., Gottshall, K. R., Hunter, J. J., Chien, K. R., and Ross, J., Jr. (1996) *Circulation* **94,** 1109–1117
35. Broberg, C. S., Pantely, G. A., Barber, B. J., Mack, G. K., Lee, K., Thigpen, T., Davis, L. E., Sahn, D., and Hohimer, A. R. (2003) *J. Am. Soc. Echocardiogr.* **16,** 814–823
36. Saraste, A., Kytö, V., Saraste, M., Vuorinen, T., Hartiala, J., and Saukko, P. (2006) *Am. J. Physiol. Heart Circ. Physiol.* **291,** H871–875
37. Ohta, K., Nakajima, T., Cheah, A. Y., Zaidi, S. H., Kaviani, N., Dawood, F., You, X. M., Liu, P., Husain, M., and Rabinovitch, M. (2004) *Am. J. Physiol. Heart Circ. Physiol.* **287,** H286–292
38. Hayashidani, S., Tsutsui, H., Ikeuchi, M., Shiomi, T., Matsusaka, H., Kubota, T., Imanaka-Yoshida, K., Itoh, T., and Takeshita, A. (2003) *Am. J. Physiol. Heart Circ. Physiol.* **285,** H1229–1235
39. Matsumura, S., Iwanaga, S., Mochizuki, S., Okamoto, H., Ogawa, S., and Okada, Y. (2005) *J. Clin. Invest.* **115,** 599–609
40. Creemers, E. E., Davis, J. N., Parkhurst, A. M., Leenders, P., Dowdy, K. B., Hapke, E., Hauet, A. M., Escobar, P. G., Cleutjens, J. P., Smits, J. F., Daemen, M. J., Zile, M. R., and Spinale, F. G. (2003) *Am. J. Physiol. Heart Circ. Physiol.* **284,** H364–371
41. Ikonomidis, J. S., Hendrick, J. W., Parkhurst, A. M., Herron, A. R., Escobar, P. G., Dowdy, K. B., Stroud, R. E., Hapke, E., Zile, M. R., and Spinale, F. G. (2005) *Am. J. Physiol. Heart Circ. Physiol.* **288,** H149–158
42. Tian, H., Cimini, M., Fedak, P. W., Altamentova, S., Fazel, S., Huang, M. L., Weisel, R. D., and Li, R. K. (2007) *J. Mol. Cell Cardiol.* **43,** 733–743
43. Kassiri, Z., and Khokha, R. (2005) *Thromb. Haemost.* **93,** 212–219